Thin Film Diblock Copolymers in Electric Field: Transition from Perpendicular to Parallel Lamellae

Yoav Tsori and David Andelman*

School of Physics and Astronomy, Raymond and Beverly Sackler Faculty of Exact Sciences, Tel Aviv University, 69978 Ramat Aviv, Israel

ABSTRACT: We examine the alignment of thin film diblock copolymers subject to a perpendicular electric field. Two regimes are considered separately: weak segregation and strong segregation. For weakly segregated blocks and below a critical value of the field, E_c, surface interactions stabilize stacking of lamellae in a direction parallel to the surfaces. Above the critical field, a first-order phase transition occurs when lamellae in a direction perpendicular to the confining surfaces (and parallel to the field) become stable. The film morphology is then a superposition of parallel and perpendicular lamellae. In contrast to Helfrich−Hurault instability for smectic liquid crystals, the mode that gets critical first has the natural lamellar periodicity. In addition, undulations of adjacent intermaterial dividing surfaces are out-of-phase with each other. For diblock copolymers in the strong segregation regime, we find two critical fields E_1 and $E_2 > E_1$. As the field is increased from zero above E_1, the region in the middle of the film develops an orientation perpendicular to the walls, while the surface regions still have parallel lamellae. When the field is increased above E_2, the perpendicular alignment spans the whole film. In another range of parameters, the transition from parallel to perpendicular orientation is direct.

1. Introduction

Diblock copolymers are known to self-assemble into a variety of ordered structures, with a length scale ranging from nanometers to micrometers. These phases have potential applications in nanolithographic templates,[1] waveguides,[2] and dielectric mirrors.[3] The length scale and morphology in the melt can easily be adjusted by controlling the fraction $f = N_A/N$ of A monomers in an A/B chain of $N = N_A + N_B$ monomers and the temperature T.[4−6]

In experiments one often encounters samples in the lamellar phase (made up of alternating planar A- and B-rich domains) in which the melt is only partially ordered. Ordered microdomains, or grains (typical size in the micrometer range), with grain boundaries between them are defects that cost energy. To anneal these defects and to create a perfect alignment of the lamellae, several techniques have been used. In the bulk, mechanical shear proved to be a successful technique. Alignment by application of an electric field[7−10] is also possible, but for macroscopic samples it requires a high-voltage difference between the two bounding electrodes. Nevertheless, this technique is especially suitable for thin films, because the thickness involved makes the required large fields (typically 10−30 V/μm) accessible.

We consider in this paper thin films of lamellar diblock copolymers, under the influence of a perpendicular electric field. Initially, the lamellae are parallel to the confining surfaces, because of preferential short-range interactions with the surfaces. In section 2 we consider diblock copolymers in the weak segregation regime. We show in section 3 that electric field applied perpendicular to the surfaces can cause the melt to transform from a parallel to a perpendicular orientation through a first-order phase transition. The critical field E_c for this transition is caused by a competition between the electric field and surface interactions. In section 4 we investigate the thin-film alignment for diblocks in the strong segregation regime. In this regime, the

surface correlations are finite, and thus the range of parallel ordering induced by the surfaces is finite as well. We give the transitions between parallel, perpendicular, and mixed lamellae in terms of the system parameters, using a phenomenological model. In both weak and strong segregation regimes, large distortions are present in the copolymer film, and these could be observed in experiments.

2. Weakly Segregated Lamellae

The copolymer order parameter $\phi(\mathbf{r}) = \phi_A(\mathbf{r}) - f$ is the deviation of the A monomer local volume fraction from its average f. Above the order−disorder transition (ODT) temperature, the melt is in the disordered, homogeneous state, with $\phi(\mathbf{r}) = 0$. As the temperature is reduced below the ODT temperature, the system goes through a first-order phase-transition to the lamellar phase provided that $|f - \frac{1}{2}|$ is small enough. Close to the ODT temperature and in the single-mode approximation, the block copolymer (BCP) order parameter is then given by

$$\phi(\mathbf{r}) = \phi_L \cos(\mathbf{q}_0 \cdot \mathbf{r}) \tag{1}$$

where $d_0 = 2\pi/q_0$ is the period of lamellar modulations and ϕ_L is their amplitude (to be determined later).

Consider a copolymer melt below the ODT confined by two flat parallel surfaces at $y = \pm\frac{1}{2}L$, as in Figure 1. The surfaces reduce chain entropy but also chemically interact with the polymers. The difference in the A- and B-block surface interactions, σ_{AS} and σ_{BS}, defines the parameter σ,

$$\sigma = \sigma_{AS} - \sigma_{BS} \tag{2}$$

In general, $\sigma(x,y)$ can be different for the two surfaces, and hence σ^+ is defined on the $y = \frac{1}{2}L$ surface and σ^- is defined for $y = -\frac{1}{2}L$. The surface interaction, F_s, can be written as an integral over the bounding surfaces
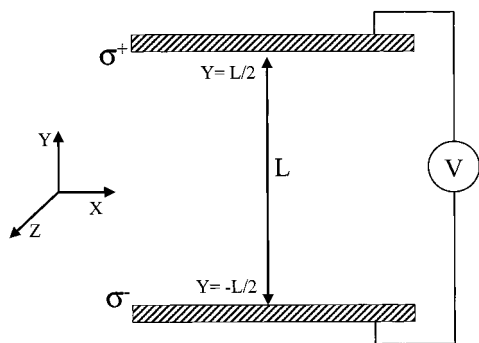
Figure 1. Schematic illustration of the system. The two confining surfaces are at $y = \pm^1/_2 L$ and have surface interaction parameters $\sigma^\pm$. The electric field points in the perpendicular y direction and is produced by a potential difference V between the two surfaces (electrodes).

(in units of $k_B T$)

$$F_s = \int \{\sigma^- \phi^- + \sigma^+ \phi^+\} \, dx \, dz \qquad (3)$$

where $\phi^- = \phi(y = -^1/_2 L)$ and $\phi^+ = \phi(y = ^1/_2 L)$. Terms that do not depend on the copolymer order parameter are not important to subsequent calculations and were dropped out. The interaction in eq 3 is short-range, localized at the surfaces. A positive $\sigma^\pm > 0$ induces adsorption of the B monomers ($\phi^\pm < 0$), and $\sigma^\pm < 0$ induces the adsorption of the A monomers ($\phi^\pm > 0$). We restrict ourselves to homogeneous surfaces, for which $\sigma^\pm$ are taken to be constants over each of the two surfaces.

First let us consider a BCP film without an external electric field. We have already considered this case in a previous publication[11] and briefly review here the BCP behavior. If the surface affinities $\sigma^\pm$ are sufficiently large, the lamellae will order in a parallel arrangement. These lamellae stretch or compress, increasing the bulk free energy, to decrease surface energy. We use below an adaptation of the strong stretching approximation used by Turner[12] and Walton et al.[13] to describe these lamellae. The lamellar period is $d_0 = 2\pi/q_0$, and m is the closest integer to L/d_0. Depending on the values of $\sigma^\pm$, an integer ($n = m$) or half-integer ($n = m + ^1/_2$), a number of lamellae exist between the two surfaces. In the former case the ordering is symmetric (the same type of monomers wet both surfaces), while in the latter it is antisymmetric (A monomers wet one surface, whereas B monomers wet the other surface). The parallel lamellae are described by an order parameter $\phi_\parallel$ given by[11]

$$\phi_\parallel(y) = \pm\phi_L \cos\left[q_\parallel\left(y + \frac{1}{2}L\right)\right] \qquad (4)$$

The wavenumber is $q_\parallel = 2\pi n/L$, and the choice of $\pm$ sign in eq 4 is such that the surface interactions, eq 3, are minimized. The amplitude of sinusoidal modulations ϕ_L is equal to the amplitude of density modulations in a bulk system and is given below in eq 13.

We consider now the case where an electric field is turned on, in a direction that is perpendicular to the surfaces (y-axis in Figure 1). Under conditions of constant voltage difference across the electrodes situated at the two bounding surfaces, the minimum of the free energy is obtained by maximizing the capacitance. Noting that since the A- and B-monomers (blocks) have different dielectric constants, the effect of the electric

field is to align the BCP layers parallel to the field, i.e., perpendicular to the surfaces. At a certain field strength, E_c, this tendency balances the preference for parallel lamellae as induced by the surfaces. Further increase of E above the critical value E_c gives rise to a perpendicular lamellar ordering.

Close to the ODT, the copolymer ordering is weak, and the energetic cost of compressing or bending the lamellae is small. In this regime the intermaterial dividing surface (IMDS) of the lamellar phase, given by the requirement $\phi(\mathbf{r}) = ^1/_2 - f$, can be substantially perturbed from its flat state. This reasoning leads us to the following superposition ansatz. For zero electric field E, surface interactions orient the lamellae in a parallel orientation. The order parameter is then given by $\phi(\mathbf{r}) = w(E{=}0)\phi_\parallel(y)$. The dimensionless amplitude $w > 0$ is determined by the strength of the surface interactions and can be larger than unity if $\sigma^\pm$ are sufficiently large. Namely, the surface-induced order can be stronger than in the bulk. Upon increase of the electric field, the function $w(E)$ of this parallel state diminishes, while the function $g(E)$ of perpendicular lamellae (parallel to the electric field) increases. This can be modeled by using the superposition ansatz for the order parameter $\phi(\mathbf{r}, E)$ in the presence of the field E:

$$\phi(\mathbf{r}, E) = w(E) \, \phi_\parallel(\mathbf{r}) + g(E) \, \phi_\perp(\mathbf{r}) \qquad (5)$$

The order parameter of the perpendicular lamellae is $\phi_\perp(x)$. It depends only on the wavenumber $q_\perp$ and is given in the single-mode approximation (weak segregation) by

$$\phi_\perp(\mathbf{r}) = \phi_\perp(x) = \phi_L \cos(q_\perp x) \qquad (6)$$

The wavenumber $q_\perp$ is yet to be determined. Without the electric field, $E = 0$, the amplitude of perpendicular modulations vanishes, $g = 0$. As the limit $E \to \infty$ is approached, the effect of the confining surfaces becomes negligible, and the BCP ordering is given by the bulk perpendicular lamellae $\phi_\perp$ ($g = 1$). Hence, the weight amplitudes $w(E)$ and $g(E)$ satisfy the following limits as a function of E:

$$g(E{=}0) = 0, \quad g(E{=}\infty) = 1 \qquad (7)$$

$$w(E{=}0) = \text{const}, \quad w(E{=}\infty) = 0 \qquad (8)$$

To get explicit expression for the weight functions w and g, we need to consider a specific model. The free energy we use in this section is applicable to the weak segregation regime and is given by $\mathcal{F} = \mathcal{F}_b + \mathcal{F}_s$,[14-16] with $\mathcal{F}_s$ from eq 3 and $\mathcal{F}_b$ being the bulk contribution. This part of the free energy has a polymer (nonelectrostatic) and electrostatic contributions (in units of $k_B T$),

$$\mathcal{F}_b = \mathcal{F}_p + \mathcal{F}_{el} \qquad (9)$$

Hereafter, we restrict ourselves to symmetric ($f = ^1/_2$) diblock copolymers, where the polymer part of the free energy is[4,14-18]

$$\mathcal{F}_p = \int \left\{ \frac{1}{2}\tau\phi^2 + \frac{1}{2}h(q_0^2\phi + \nabla^2\phi)^2 + \frac{u}{24}\phi^4 \right\} d^3r \qquad (10)$$

The parameters in eq 10 are given by

$$q_0 = 1.95/R_g; \quad h = 3\rho c^2 R_g^2/2q_0^2 \qquad (11)$$

$$\chi_c \simeq 10.49/N; \quad \tau = 2\rho N(\chi_c - \chi) \qquad (12)$$

Denoting b as the monomer size, the radius of gyration for Gaussian chains is $R_g^2 \simeq \frac{1}{6}Nb^2$. The polymerization index is N, the chain density of an incompressible melt is $\rho = 1/Nb^3$, and χ is the Flory parameter. The amplitude ϕ_L in the parallel and perpendicular states is

$$\phi_L^2 = -8\tau/u, \quad \tau < 0 \qquad (13)$$

as is obtained by inserting eq 1 in $\mathcal{F}_p$ of eq 10 and minimizing with respect to ϕ_L. The dimensionless ratio u/ρ and c are of order unity and are taken to be equal exactly to one in the remaining of the paper, $u/\rho = c = 1$. The correlation length $\xi \equiv 2q_0^2(|\tau|/h)^{-1/2}$ is assumed to be larger than the film thickness, $\xi \gtrsim L$.[19]

The electrostatic contribution in units of $k_B T$ is[7,20]

$$\mathcal{F}_{el} = \beta \int (\hat{\mathbf{q}} \cdot \mathbf{E})^2 \phi_{\mathbf{q}} \phi_{-\mathbf{q}} \, d^3 \mathbf{q} \qquad (14)$$

$$\beta = \frac{(\epsilon_A - \epsilon_B)^2}{4(2\pi)^4 k_B T \langle \epsilon \rangle} \qquad (15)$$

Here $\phi_{\mathbf{q}}$ is the Fourier transform of $\phi(\mathbf{r})$: $\phi(\mathbf{r}) = \int \phi_{\mathbf{q}} \exp(i\mathbf{q} \cdot \mathbf{r}) \, d\mathbf{q}$, and $\hat{\mathbf{q}} = \mathbf{q}/q$ is a unit vector in the $\mathbf{q}$-direction. Copolymer modulations with a nonvanishing component of the wavenumber $\mathbf{q}$ along the electric field have a positive contribution to the free energy. In other words, there is a free energy penalty for having dielectric interfaces in a direction perpendicular to the electric field. In eq 15, ϵ_A and ϵ_B are the dielectric constants of the pure A- and B-blocks, respectively,[7,8] and $\langle \epsilon \rangle$ is the material average dielectric constant for the BCP film,

$$\langle \epsilon \rangle = f\epsilon_A + (1 - f)\epsilon_B \qquad (16)$$

Throughout the remainder of this paper we will focus only on symmetric melts ($f = \frac{1}{2}$), having an average dielectric constant $\langle \epsilon \rangle = \frac{1}{2}(\epsilon_A + \epsilon_B)$. For small concentration variations, valid in the weak segregation regime, ϵ varies linearly with the local copolymer composition ϕ,

$$\epsilon(\phi) = \left(\frac{1}{2} + \phi\right)\epsilon_A + \left(\frac{1}{2} - \phi\right)\epsilon_B$$

$$= \langle \epsilon \rangle + (\epsilon_A - \epsilon_B)\phi \qquad (17)$$

It is possible to perform the spatial integration in eqs 3, 10, and 14, yielding the free energy per unit volume $F = F_p + F_{el} + F_s$ for a general order parameter $\phi(\mathbf{r})$, eq 5:

$$F = \frac{1}{4}\phi_L^2[(\tau + C_\parallel(E))w^2 + (\tau + C_\perp)g^2] + \frac{u\phi_L^4}{64}(w^4 +$$

$$g^4) + \frac{u\phi_L^4}{16}w^2g^2 + \frac{w\Sigma}{L} \qquad (18)$$

The quantities $C_\parallel$ and $C_\perp$ are positive and given by

$$C_\parallel(E) = h(q_0^2 - q_\parallel^2)^2 + 2\beta E^2 \qquad (19)$$

$$C_\perp = h(q_0^2 - q_\perp^2)^2 \qquad (20)$$

$\Sigma = \pm \phi_L \sigma^- \pm \phi_L \sigma^+$ is related to the surface interaction and is negative. The $\pm$ sign is determined from the $\pm$ sign of the order parameter in eq 4. The free energies $F_\parallel$ and $F_\perp$ of the parallel and perpendicular states, respectively, are given as limiting cases

$$F_\parallel = F(w, g{=}0) = \frac{1}{4}\phi_L^2[\tau + C_\parallel(E)]w^2 + \frac{u\phi_L^4}{64}w^4 + \frac{w\Sigma}{L} \qquad (21)$$

$$F_\perp = F(w{=}0, g{=}1) = \frac{1}{4}\phi_L^2(\tau + C_\perp) + \frac{u\phi_L^4}{64} \qquad (22)$$

As discussed in the Introduction, we concentrate on the interesting case where in the absence of electric field the BCP has a parallel ordering given by $\phi = w\phi_\parallel$ (with some weight w). This is equivalent to saying that there exist w such that $F_\parallel(E{=}0) < F_\perp(E{=}0)$. By inserting $E = 0$ and $q_\perp = q_0$ in eqs 21 and 22, we get that in this case

$$\frac{1}{4}\phi_L^2[\tau + C_\parallel(0)]w^2 + \frac{u\phi_L^4}{64}w^4 + \frac{w\Sigma}{L} < -\frac{\tau^2}{u} \qquad (23)$$

Therefore, the free energy of the parallel lamellae is expected to be lower than the free energy of the perpendicular lamellae. This assumption is valid for strong enough surface interactions, Σ. In the next section we proceed to find the weight functions $w(E)$ and $g(E)$ for any $E > 0$.

3. Results of the Weak Segregation Model

The free energy (eq 18) is minimized with respect to w and g to yield two coupled algebraic equations:

$$(\tau + C_\perp)g - \tau g^3 - 2\tau w^2 g = 0 \qquad (24)$$

$$[\tau + C_\parallel(E)]w - \tau w^3 - 2\tau g^2 w + 2\Sigma/L\phi_L^2 = 0 \qquad (25)$$

As we will see below, there is a critical value of the electric field, E_c, which separates between the small and large field behavior. One can estimate E_c as the field in which the bulk electrostatic energy $\sim LE^2$ (favoring perpendicular lamellae) balances the surface interactions Σ, and hence $E_c \sim L^{-1/2}$.

Equations 24 and 25 are analyzed separately for small and large electric fields.

(i) Small Electric Fields: $E < E_c$. For zero electric field, the lamellae are in their parallel state, namely $g = 0$. The solution with $g(E) = 0$ and $w(E) \neq 0$ (in eqs 24 and 25) corresponds to the minimum of the free energy if E is below a certain threshold value E_c, which is to be determined later. Denoting $g_<(E)$ and $w_<(E)$ as the weight amplitudes for electric fields $E < E_c$, they satisfy the following equations:

$$g_<(E) = 0 \qquad (26)$$

$$[\tau + C_\parallel(E)]w_<(E) - \tau w_<^3(E) + 2\Sigma/L\phi_L^2 = 0 \qquad (27)$$
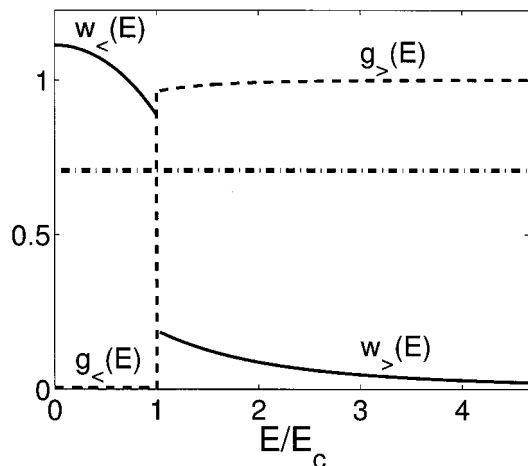
Figure 2. Weight functions $w(E)$ and $g(E)$. The horizontal dash–dot line $w = 1/\sqrt{2}$ is the value of w below which a nonzero $g(E)$ is possible. Surface separation is $L = 8d_0$ and the Flory parameter is $N\chi = 11$. The film is symmetric, $\sigma^+ = \sigma^- = 0.6hq_0^3\phi_L$.

(ii) Large Electric Fields: $E > E_c$. There is a solution to eqs 24 and 25 with perpendicular lamellae, namely with a nonzero $g(E)$. This solution gives the minimum of the free energy above a critical field, $E > E_c$. The weight amplitudes $g_>(E)$ and $w_>(E)$ are then given by

$$g_>^2(E) = \frac{\tau + C_\perp}{\tau} - 2w_>^2(E) \geq 0 \qquad (28)$$

$$(-\tau + C_\parallel(E) - 2C_\perp)\,w_>(E) + 3\tau w_>^3(E) + 2\Sigma/L\phi_L^2 = 0 \qquad (29)$$

The above solution is valid provided that $w_>$ is small enough, as given by the inequality

$$w_>^2(E) \leq \frac{1}{2} + \frac{C_\perp}{2\tau} \leq \frac{1}{2} \qquad (30)$$

Since $w(E)$ is a decreasing function, from eq 20 we see that increasing the electric field E from zero, the natural mode of the perpendicular state, $q_\perp = q_0$, is the first to become critical. Namely, the inequality above is obeyed first when $q_\perp$ is equal to the bulk mode q_0 and only later by other q-modes. For this reason we assume hereafter that $q_\perp = q_0$, yielding $C_\perp = 0$ and $g_>^2(E) = 1 - 2w_>^2(E)$. Thus, BCP modulations in a direction parallel to the surfaces have the bulk (free) periodicity d_0.

Equation 29 is a cubic equation for $w_>$ and has an analytical solution. It is convenient to express the solution via a parameter θ defined as

$$\cos[\theta(E)] \equiv -\frac{\Sigma/L\phi_L^2}{3\tau}\left(\frac{\tau - C_\parallel(E)}{9\tau}\right)^{-3/2} < 0 \qquad (31)$$

and take it to be in the range $\pi < \theta < {}^3/_2\pi$. Recalling that Σ and τ are negative, the solution $w_>$ to eq 29 is then simply given by

$$w_>(E) = 2\sqrt{\frac{\tau - C_\parallel(E)}{9\tau}}\,\cos\!\left(\frac{\theta}{3}\right) \qquad (32)$$

Curves of $g(E)$ and $w(E)$ are shown in Figure 2 within the assumption $q_\perp = q_0$. For zero electric field, the film
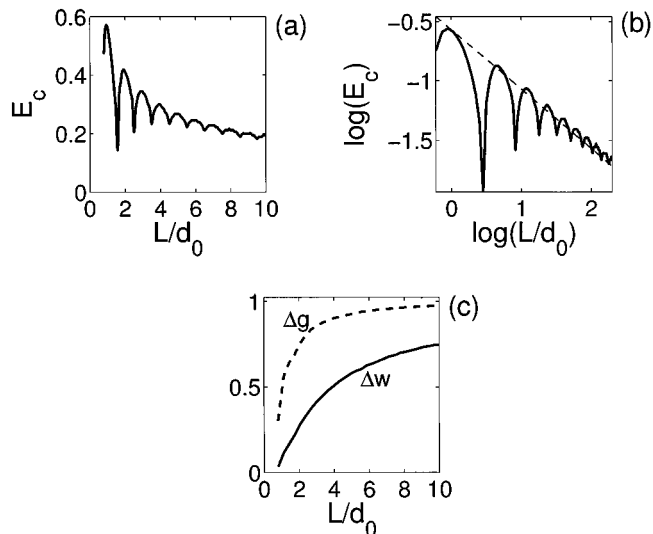
Figure 3. (a) Critical field E_c [in units of $(hq_0^4/\beta)^{1/2}$] required for the appearance of perpendicular lamellae, as a function of surface separation L. (b) A log–log plot of the same curve as in part a. The dashed line is a straight line corresponding to $E_c \approx 0.5(L/d_0)^{-1/2}$ (see text). (c) The jumps Δg (dashed line) and Δw (solid) in the amplitudes g and w at the critical field E_c, as a function of surface separation L. The film is symmetric, and $\sigma^\pm$ and $N\chi$ are as in Figure 2.

has parallel lamellae, $g(0) = 0$. With increasing electric field E, the amplitude $w_<(E)$ of parallel lamellae decreases monotonically, as is given by eq 27, while $g_<(E)$ remains zero. At the critical field, $E = E_c$, there is a first-order phase transition, and perpendicular lamellae appear. The weight amplitudes $w(E)$ and $g(E)$ are discontinuous; the jump in their values is determined by the degree of segregation $N\chi$, intersurface separation L, and surface parameters $\sigma^\pm$. Further increase of the electric field causes $g(E)$ to increase while $w(E)$ decreases. For very large electric fields, $E \to \infty$, the perpendicular state saturates to its value $g = 1$, and parallel lamellae completely disappear, $w = 0$.

The critical field E_c is determined by the condition

$$F(w_<,\ g_<) = F(w_>,\ g_>) \qquad (33)$$

where the free energy F is taken from eq 18. Namely, it is the field where the two values of the free energy cross. The critical field E_c as a function of surface separation L is shown in Figure 3 a for weak segregations ($N\chi = 11$). As the surface separation L increases, E_c decreases with typical oscillations of period d_0. These oscillations are caused by the frustration occurring when the surface separation is incommensurate with the lamellar period. Figure 3b shows a log–log plot of the same curve. The dashed line shows a fit to a $E_c \sim L^{-1/2}$ scaling. This scaling can be obtained by balancing the surface energy Σ with the electrostatic contribution $\sim LE_c^2$. There is good fit between this $L^{-1/2}$ line and the peak positions, as expected for unstrained films.[21] However, for frustrated films (where the film thickness is incommensurate with the lamellar period) the deviation from $E_c \sim L^{-1/2}$ becomes increasingly important as the surface separation L is reduced below roughly $6d_0$ for the parameters used.

We define $w_<^\ell$ as the value of w just before the transition ($E \uparrow E_c$) and $w_>^\ell$ as the value after the transition ($E \downarrow E_c$), and similarly for g. The jump in the
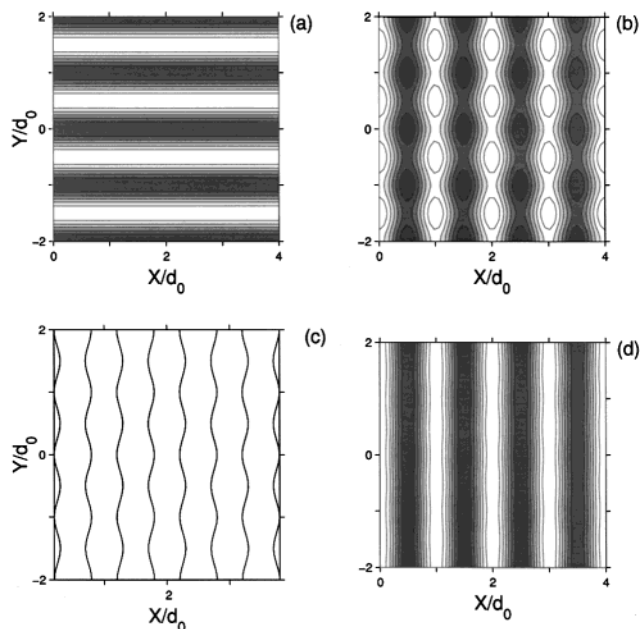
Figure 4. Contour plots of the BCP order parameter $\phi(x,y) = w(E)\phi_{\parallel}(y) + g(E)\phi_{\perp}(x)$ for symmetric film. The surfaces are at $y = \pm^{1}/_{2}L = \pm 2d_{0}$, and the field is in the y direction. In part a the field is a little smaller than the critical field, $E = 0.98E_{c}$, and the film has a perfect parallel ordering. In part b the field is just above the threshold, $E = 1.02E_{c}$. The film morphology is a superposition of parallel and perpendicular lamellae. (c) A plot of the IMDS [given by $\phi(x,y) = 0$] of part b. In part d $E = 4E_{c}$, and the lamellae are in the perpendicular state with small distortions. The surface fields are $\sigma^{+} = \sigma^{-} = 0.5hq_{0}{}^{3}\phi_{L}$, and the Flory parameter is $N\chi = 11$ corresponding to correlation length $\xi \simeq 4.8d_{0} > L$. The B monomers (colored black) are attracted to the two symmetric surfaces.

weight amplitudes Δw and Δg is

$$\Delta w = |w_{>}^{c} - w_{<}^{c}| \qquad (34)$$

$$\Delta g = g_{>}^{c} - g_{<}^{c} = g_{>}^{c} \qquad (35)$$

These quantities are plotted as a function of surface separation L in Figure 3c, for the same parameters as in Figure 3a. As L increases, the critical field E_{c} decreases, the jump in w and g gets larger, and the transition from parallel to perpendicular lamellae becomes more abrupt.

In Figure 4 we show how the film changes its orientation and morphology as the electric field increases. In part a, we show a contour plot of the copolymer order parameter $\phi = w(E)\phi_{\parallel} + g(E)\phi_{\perp}$, for $E < E_{c}$, but only slightly below it. The ordering in the film is parallel to the surfaces, as $g(E) \equiv 0$. In part b, the field is slightly increased above its threshold value E_{c}, and the undulations created by the appearance of the perpendicular state are prominent. In contrast to the classical Helfrich−Hurault undulations[22] calculated for smectic and cholesteric liquid crystals, here the lateral wavelength is finite and is equal to the free periodicity d_{0}. Note that the correlation length ξ is larger than the film thickness, $\xi > L$. In addition, the modulations of the adjacent intermaterial dividing surfaces (IMDS), given by $\phi(\mathbf{r}) = 0$, are shown in part c to be out-of-phase with each other and are pronounced only for $E \simeq E_{c}$. Although the perpendicular ordering may be very strong, some parallel ordering is still
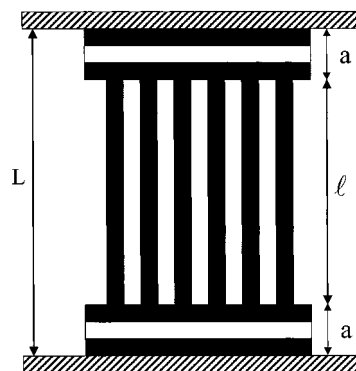
Figure 5. Illustration of the lamellae in the film in the strong segregation regime. A region with perpendicular lamellae exists in the middle of the film, with size l. Two regions of size a each are the parallel lamellar regions.

present (finite $w > 0$). As the electric field is further increased, there is only little reminiscence of the parallel ordering, and the perpendicular lamellae are nearly perfect. This can be seen in Figure 4d, where we choose $E = 4E_{c}$.

4. Strongly Segregated Lamellae

In this section we consider the same alignment phenomenon under an electric field as in the previous section, but the BCP melt is assumed to be in the strong segregation limit, i.e., $N\chi \gg N\chi_{c} \simeq 10.5$. In this regime the lamellae are not easily deformed, and the effect of the surface field is important only close to the confining walls, in contrast to the long-range ordering induced by the surfaces in the weak segregation.

4.1. Unstrained Films. We discuss first the alignment phenomenon ignoring the effect of incommensurability between the film thickness L and the free lamellar period d_{0}. In the following section generalization to strained films will be presented as well. For simplicity, we also assume that the two walls are chemically identical and preferring the B monomers: $\sigma_{BS} < \sigma_{AS}$, $\sigma^{\pm} > 0$. For sufficiently strong E fields we expect to nucleate a region in the middle of the film with lamellae perpendicular to the walls, as is shown schematically in Figure 5. Hence, two regions of a "T-junction" morphology will exist in the film, in the vicinity of the bounding surfaces. A positive energy penalty (per unit area) γ_{T} is associated with each of the two T-junction defects. In principle, other types of defects might exist in the film, but this can only affect the value of γ_{T} and not the system behavior as is described below.

We denote the size of the region that is perpendicular to the surfaces by l. If $l = 0$, the film has only parallel ordering, while for $l = L$ the perpendicular ordering spans the whole film. The free energies per unit area, $F_{\parallel}$ and $F_{\perp}$, for these two extreme cases are

$$F_{\parallel} = LF_{p} + 2\sigma_{BS} - \lambda_{\parallel}LE^{2} \qquad (36)$$

$$F_{\perp} = LF_{p} + \sigma_{AS} + \sigma_{BS} - \lambda_{\perp}LE^{2} \qquad (37)$$

F_{p} is the polymer free energy per unit volume of a BCP in the lamellar phase, and in the above we have used two different depolarization factors, $\lambda_{\parallel}$ and $\lambda_{\perp}$, for the
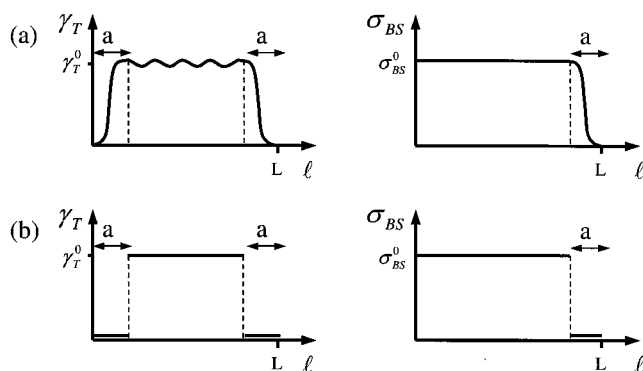
Figure 6. (a) Qualitative dependence of γ_T and σ_{BS} on the thickness of perpendicular domain l, defined in Figure 5. (b) Simplified curves of part a. The cutoff width is a, the total film thickness is L, and γ_T^0 and σ_{BS}^0 are the mean values of γ_T and σ_{BS}, respectively, for $a < l < L - a$.

two orientations

$$\lambda_{\parallel} = \frac{1}{4\pi} \frac{\epsilon_A \epsilon_B}{\epsilon_A + \epsilon_B}$$

$$\lambda_{\perp} = \frac{1}{16\pi}(\epsilon_A + \epsilon_B) \tag{38}$$

These two depolarization factors can be obtained by calculating the electrostatic energy $-(8\pi)^{-1}\int\epsilon E^2 \, d^3r$ of the film and using the boundary condition that the displacement field $D = \epsilon E$ is continuous across the two dielectric boundaries. Note that $\lambda_{\perp} > \lambda_{\parallel}$, meaning that $-\lambda_{\perp}E^2 < -\lambda_{\parallel}E^2$, and the perpendicular state is favored for $E \to \infty$.

Let us focus on the mixed state as is illustrated in Figure 5. For intermediate values of l, $0 < l < L$, there are two surface regions of parallel orientation and a central region of perpendicular orientations. The free energy of this mixed state F_M (per unit area) is

$$F_M = LF_p + 2\sigma_{BS} + 2\gamma_T - \lambda_m(l)LE^2 \tag{39}$$

The system can be regarded as being composed of two capacitors of parallel lamellae and one capacitor of perpendicular lamellae connected in series, yielding the constant $\lambda_m(l)$

$$\lambda_m(l) = \left[\frac{L-l}{L\lambda_{\parallel}} + \frac{l}{L\lambda_{\perp}}\right]^{-1} \tag{40}$$

We note that a similar expression for the electrostatic part of the mixed state free energy was previously derived by Pereira and Williams.[21]

The value of the surface energies σ_{AS}, σ_{BS}, and γ_T must depend on l. To see this, consider, for example, $L \gg d_0$ and $l = \frac{1}{2}L$. In this case γ_T is some constant. But as $l \to L$, the value of γ_T must approach zero, because when $l = L$, the T-junction does not exist, and the energy associated with it is zero. We denote by a the cutoff length, which is the characteristic width at which γ_T goes to zero. From the same reason γ_T must also tend to zero as $l \to 0$, with another cutoff length. For simplicity, we assume that this cutoff length is also equal to a. Similarly, the surface interaction energies σ_{AS} and σ_{BS} tend to zero as $l \to L$, with the same cutoff length. The qualitative forms of these parameters are shown in Figure 6a. The smooth monotonic decay to zero

at $l = L$ and $l = 0$ is only suggestive. $\gamma_T(l)$ has oscillations with period $\frac{1}{2}d_0$.

In principle, one should minimize F_M with respect to the size of perpendicular domain l. This generalized (mixed) state would correspond to the parallel state when the minimum is at $l = 0$ and to the perpendicular state when the minimum is at $l = L$. However, we do not know from a molecular description how σ_{AS}, σ_{BS}, and γ_T fall off to zero and therefore use the approximation shown in Figure 6b. $\sigma_{AS}(l) = \sigma_{AS}^0$ and $\sigma_{BS}(l) = \sigma_{BS}^0$ are constant for $l < L - a$ and zero for $l > L - a$. $\gamma_T(l) = \gamma_T^0$ is constant in the range $a < l < L - a$ and zero otherwise. To make the notation simpler, we drop hereafter the superscript zero of σ_{AS}, σ_{BS}, and γ_T. Note that the effect of incommensurability between the surface spacing L and the lamellar period d_0 appears as undulations in the plot of $\gamma_T(l)$ (Figure 6a), and these undulations are neglected here and will be addressed below separately.

With the above assumptions, the size l of a perpendicular domain that minimizes the mixed free energy F_M is $l = L - 2a$. The free energy of the mixed configuration is thus taken from eq 39 with λ_m given by

$$\lambda_m = \left[\frac{2a}{L\lambda_{\parallel}} + \frac{L-2a}{L\lambda_{\perp}}\right]^{-1} \tag{41}$$

Using the assumption that the B-polymer is adsorbed at the surfaces in the parallel state ($\sigma_{BS} < \sigma_{AS}$), we plot in Figure 7 $F_{\parallel}$, $F_{\perp}$, and F_M as a function of electric field strength E. The dimensionless parameter δ measuring the difference in A- and B-block surface interactions is defined as

$$\delta \equiv \frac{\sigma}{\gamma_T} = \frac{\sigma_{AS} - \sigma_{BS}}{\gamma_T} \tag{42}$$

On the basis of the value of δ, we now discuss two cases:

(i) Strong Surface Fields: $\delta > \delta^*$. If δ is larger than a threshold value δ^*, given by

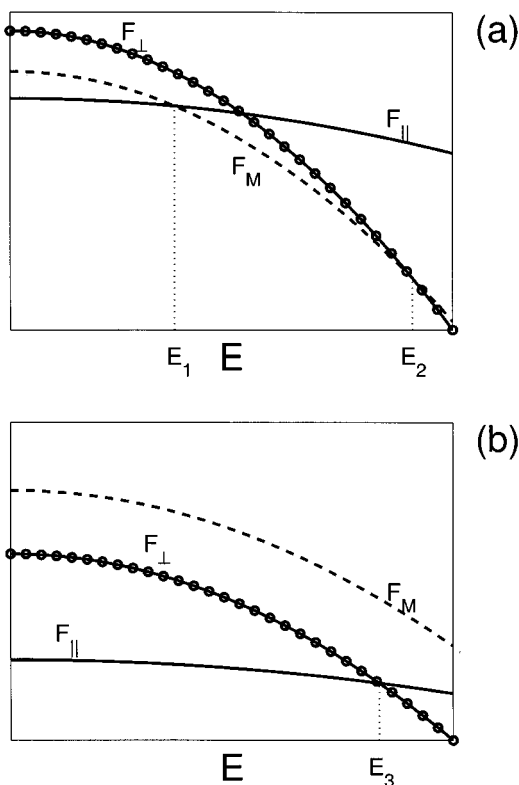$$\delta^* \equiv 2\frac{\lambda_{\perp} - \lambda_{\parallel}}{\lambda_m - \lambda_{\parallel}}$$

$$= 2 + \frac{4\lambda_{\perp}}{\lambda_{\parallel}}\frac{a}{L} + O\left(\frac{a^2}{L^2}\right) \tag{43}$$

there are two distinct critical fields E_1 and $E_2 > E_1$ given by

$$E_1 = \left[\frac{2\gamma_T}{L(\lambda_m - \lambda_{\parallel})}\right]^{1/2} \tag{44}$$

$$E_2 = \left[\frac{\gamma_T(\delta - 2)}{L(\lambda_{\perp} - \lambda_m)}\right]^{1/2} \tag{45}$$

The smallest of these two fields, E_1, obtained for $F_M = F_{\parallel}$ (Figure 7a), is the field required to create the T-junction defect in the film. This field is independent of δ, and for thick films ($L \gg a$) it scales as $E_1 \sim L^{-1/2}$. For E fields in the range $E_1 < E < E_2$, the film has a

Figure 7. Sketch of the dependence of $F_\parallel$, $F_\perp$, and F_M on the field E, in solid line, circles, and dashed line, respectively. (a) $\delta > \delta^*$: There are two critical fields, obtained when $F_M(E_1) = F_\parallel(E_1)$ and $F_M(E_2) = F_\perp(E_2)$. (b) $\delta < \delta^*$: $F_M(E)$ is always larger than $F_\perp(E)$, and there is only one critical field obtained when $F_\parallel(E_3) = F_\perp(E_3)$. Above this field the most stable state is the perpendicular ordering.

region of size $l = L - 2a$ with perpendicular lamellae, while parallel lamellae are localized in a small region of size a near the two walls. The second field, E_2, obtained for $F_M = F_\perp$, is larger than E_1 and corresponds to the electric field that is required to destroy the parallel surface layer (of width a). Note that although these fields are large (typically between $1-30$ V/μm), they can be readily achieved in thin-film experiments.[10] For thick films E_2 is independent of L and obtains the asymptotic value

$$E_2 \simeq \left[\frac{\gamma_T(\delta - 2)\lambda_\parallel}{2a(\lambda_\perp - \lambda_\parallel)\lambda_\perp} \right]^{1/2} \quad (46)$$

Note also the appearance of $\lambda_m - \lambda_\parallel$ and $\lambda_\perp - \lambda_m$ in the denominator of the two critical fields in eqs 44 and 45. If the dielectric contrast between A- and B-domains is small, namely $\epsilon_A/\epsilon_B \approx 1$, then $\lambda_\parallel \approx \lambda_\perp \approx \lambda_m$, and the critical fields are large. If, on the other hand, $\epsilon_A/\epsilon_B \gg 1$, then the critical fields required to achieve mixed and perpendicular lamellae are small. For many polymer surface combinations, γ_T is large and therefore δ is small. In this case the system is classified as having weak surface fields as is discussed below.

(ii) Weak Surface Fields: $\delta < \delta^*$. For small values of δ, namely $\delta < \delta^*$, the free energies $F_\perp$ and $F_\parallel$ are always smaller than F_M. Namely, the mixed state is not a possible minimum of the film free energy. There is only one transition at a critical field E_3 occurring when
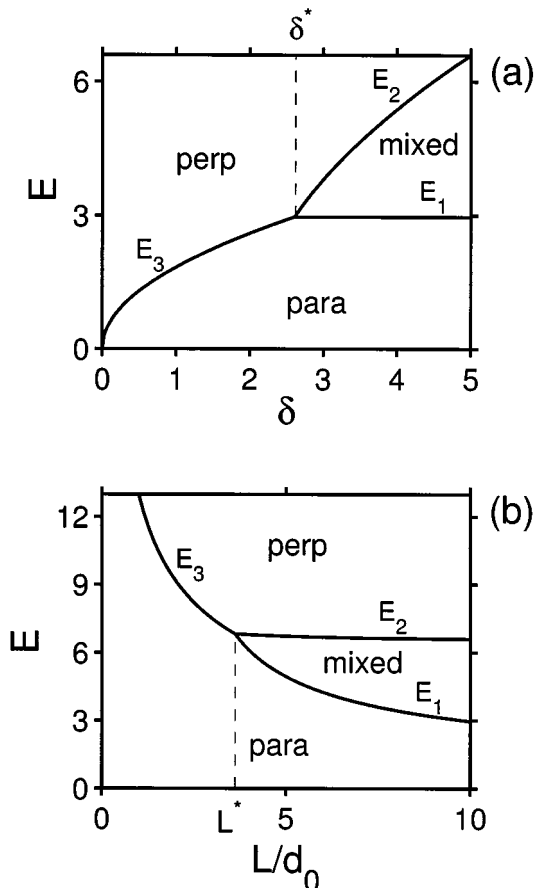
Figure 8. (a) Phase diagram in the $E-\delta$ plane. If $\delta = (\sigma_{AS} - \sigma_{BS})/\gamma_T < \delta^*$, there is a transition between parallel and perpendicular lamellae at $E = E_3$. For $\delta > \delta^*$, there is a transition from the parallel to the mixed state at $E = E_1$, followed by a second transition from the mixed to the perpendicular state when $E = E_2 > E_1$. Surface separation is chosen as $L = 10d_0$ and $a = d_0$. (b) Similar diagram, but in the $E-L$ plane, with $\delta = 5$. In both parts, the effect of mismatch between L and d_0 is neglected, and the electric fields are scaled by $(\gamma_T/d_0)^{1/2}$.

$F_\perp$ intersects $F_\parallel$ (Figure 7b). This field is given by

$$E_3 = \left[\frac{\gamma_T \delta}{L(\lambda_\perp - \lambda_\parallel)} \right]^{1/2}$$

$$= \left[\frac{\sigma}{L(\lambda_\perp - \lambda_\parallel)} \right]^{1/2} \sim \delta^{1/2} L^{-1/2} \quad (47)$$

When $E = E_3$, a direct transition occurs from a state where the whole film has parallel lamellae ($E < E_3$) to a state where the whole film has perpendicular lamellae without any surface regions ($E > E_3$).

The system behavior can be summarized in a phase diagram which depends on the three system parameters: the electric field E, the surface interaction parameter δ, and the film thickness L. In Figure 8a, we show a 2-dimensional cut through the phase diagram, varying E and δ while keeping L constant. For small electric fields, the lamellae are in the fully parallel configuration. If δ is small, a first-order phase transition to the fully perpendicular state occurs when E is increased above E_3 (eq 47). If δ is large enough, namely $\delta > \delta^*$, there are two transitions when the field is increased. In the regime $E_2 > E > E_1$, the film is in a mixed state, and layers of thickness a with parallel

lamellae still exist close to the surfaces. As E is further increased above E_2, the film has a fully perpendicular state. Note that when $\delta > \delta^*$, E_1 is the field required to initiate the T-junction defect and so is independent of σ, while E_2 is the field that destroys the surface layer, and therefore $E_2 \sim (\sigma - 2\gamma_T)^{1/2}$.

As we have seen, the condition $\delta > \delta^*$ is required for the existence of the mixed state and hence for the existence of two critical fields E_1 and E_2. Alternatively, this condition can be viewed as a restriction on the film thickness L for a given δ. Therefore, a mixed state does not exist if

$$L < L^* \equiv \frac{2a(\lambda_\perp - \lambda_\parallel)[2\lambda_\perp + (\delta - 2)\lambda_\parallel]}{\lambda_\parallel[(\delta + 2)\lambda_\perp + (\delta - 2)\lambda_\parallel]} \quad (48)$$

In the limit $\delta \gg 1$ and in the case of polystyrene ($\epsilon \approx 2.5$) and poly(methyl methacrylate) ($\epsilon \approx 6$) diblock copolymer, one obtains $L^* = 2a(\lambda_\perp - \lambda_\parallel)/(\lambda_\parallel + \lambda_\perp) \approx 1.3a$. It is smaller for smaller values of δ. Hence, the mixed state exists for film thickness larger than the range of surface-induced ordering a. We see here again why this mixed state is not be expected to occur in the weak segregation limit.

An alternative cut through the phase diagram is shown in Figure 8b, where δ is fixed while E and L are allowed to vary. For small surface separations, $L < L^*$, there is a transition from parallel to perpendicular lamellae at $E = E_3$ (eq 47). For larger separations, $L > L^*$, the mixed state appears at $E = E_1$ (eq 44). The transition to a fully perpendicular state occurs at $E = E_2$ (eq 45). The main difference between this diagram and the one obtained by Pereira and Williams[21] is that we always find the perpendicular state to be favored for large enough electric fields.

4.2. Strained Films. Strained films occur when the film thickness L does not match the lamellar period d_0; namely, L/d_0 is not an integer or a half-integer number. The effect of this mismatch, which was neglected in the previous section, is considered below. The strong segregation theory of Turner[12] and Walton et al.[13] has been successful in describing confined lamellae, and therefore we use it in this section to include the effect of lamellae frustration and to modify the free energy $F_\parallel$ from section 4.1. We use the convention that m is the closest integer to L/d_0, yielding $F_\parallel$ which is the minimum of $F_\parallel^s$ and $F_\parallel^{as}$, the symmetric and antisymmetric parallel states free energies, respectively:

$$F_\parallel^s = \sigma_{AB}\left[\left(\frac{L}{d_0}\right)^3\frac{1}{n^2} + 2n\right] + 2\sigma_{BS} - \lambda_\parallel LE^2$$

$$\text{for } n = m, \text{ symmetric} \quad (49)$$

$$F_\parallel^{as} = \sigma_{AB}\left[\left(\frac{L}{d_0}\right)^3\frac{1}{n^2} + 2n\right] + \sigma_{AS} + \sigma_{BS} - \lambda_\parallel LE^2$$

$$\text{for } n = m \pm {}^1/_2, \text{ asymmetric} \quad (50)$$

Note that in the above expressions for the free energy, eqs 49 and 50, the electrostatic part is exactly like in section 4.1. In the symmetric state, both surfaces are wetted by B monomers, while in the antisymmetric state A monomers adsorb to one surface and B monomers adsorb to the second surface.

In Figure 9 we present the phase diagrams when the mismatch between L and d_0 is taken into account, plotted with same parameters as in Figure 8. For very
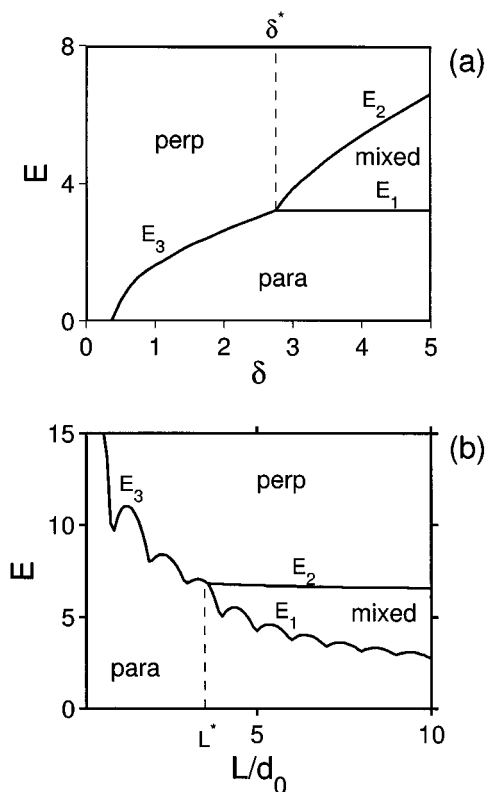
Figure 9. Phase diagrams as in Figure 8, but for strained films. The critical fields E_1 and E_3 have oscillations as a function of L, in contrast to Figure 8b, but follow on average a similar $\sim L^{-1/2}$ scaling behavior.

thin films, $L < d_0$, the perpendicular state is favored over the parallel state, even for $E = 0$. Apart from this, Figure 9a is similar to Figure 8a. However, Figure 9b is different than Figure 8b. The critical fields E_1 and E_3 separating the parallel state from the other two states have oscillations with period d_0. These curves are similar to the critical field curve for weakly segregated lamellae, Figure 3, computed in section 3, and also to the curve calculated by Ashok et al. using a similar model and different parameters.[23] Note that from the discussion of unstrained films in section 4.1 E_1 and E_3 have oscillations around lines which decay as $L^{-1/2}$ for large L. The field E_2 separating the mixed state with the perpendicular state depends only weakly on L.

5. Conclusions

In this paper we study the influence of an applied electric field on the morphology of thin film diblock copolymers. In the absence of an electric field the lamellae are taken to be ordered parallel to the confining surfaces. Strong enough E fields in the direction perpendicular to the surfaces will eventually orient the lamellae in a perpendicular direction. However, the response of weakly segregated lamellae is different than the response of strongly segregated lamellae. In the former case, the BCP order parameter is obtained as a function of electric field strength E and other system parameters (such as the degree of segregation $N\chi$, strength of surface interactions $\sigma^\pm$, and film thickness L). The field applied in the perpendicular direction diminishes the amplitude of the parallel BCP state. Above the critical field, $E > E_c$, a first-order phase transition occurs, from the parallel into the perpendicular state.

The first q-mode which becomes stable in the perpendicular state $q_\perp$ has a finite periodicity, equal to the bulk spacing $d_0 = 2\pi/q_0$. Moreover, modulations of adjacent intermaterial dividing surfaces (IMDS) are out-of-phase with each other. This is different than the strong segregation instability studied by Onuki and Fukuda,[20] where the slowly varying phase $\phi = \phi_L \cos[q_0 x + u(y)]$ is used, and the free energy is expanded in small u. At the onset of instability, they found that adjacent IMDS lines are in-phase with each other. The weak segregation IMDS undulations studied here appear because in this regime it is relatively easy to deform the lamellae. For $E > E_c$, parallel and perpendicular lamellae coexist in the film. This superposed state is yet to be verified in experiments.

The critical field E_c as a function of intersurface separation L decays with characteristic oscillations of period d_0. These oscillations are the result of lamellar frustration, occurring when the period $2\pi/q_\parallel$ is different than d_0 (while $q_\perp$ is taken always to be equal to q_0). The deviation of the critical field E_c from the $E_c \sim L^{-1/2}$ scaling (of unstrained films) is important only for small surface separations. For large L values, the $L^{-1/2}$ scaling describes well the system behavior.

The weak segregation treatment we present relies on mean-field theory. It is valid close to the critical point but not too close where critical fluctuations become important.[24] We have ignored the deviations of the intermaterial dividing surface from the perfect flat shape that occur near the surfaces. These deviations can be important for small surface separations ($L \lesssim d_0$), or close to the ODT,[15,16] and should be properly accounted for.

In the second part of the paper we consider BCP film in the strong segregation regime. In contrast to the weak segregation case, here the surface-induced ordering has a finite range of length a. This added length (taken in the weak segregation limit to be much larger than the film thickness L) results in the existence of two critical fields. Provided that the parameter δ is large enough, $\delta > \delta^*$ (eq 43), for small electric fields, $E < E_1$, the film has parallel lamellae. As the field is increased above E_1 but below E_2, a region of size $L - 2a$ of perpendicular lamellae nucleates in the middle of the film. In this mixed state, a layer of parallel lamellae of thickness equal to the cutoff length a still persists close to the surfaces. When $E > E_2$, the system is in the perpendicular state.

The full phase diagram in the $E-\delta$ and the $E-L$ planes is given in Figure 8. As discussed above, for large $\delta > \delta^*$ there is a transition from parallel to mixed lamellae at $E = E_1$ (eq 44) and from mixed to perpendicular lamellae at $E = E_2$ (eq 45). Another scenario of a direct transition from a parallel to a perpendicular state at $E = E_3$ (eq 47) is realized for small δ, $\delta < \delta^*$. These diagrams do not take into account the frustration effects caused by a mismatch between the wall separation and the natural lamellar periodicity in the bulk. In this respect, they are qualitatively applicable to nonpolymeric systems such as ferrosmectics in magnetic fields,[25] and to BCP in the hexagonal phase, as investigated experimentally.[10] The difference between the hexagonal and lamellar phase behavior comes from the different value of the depolarization factors $\lambda_\parallel$, $\lambda_\perp$, and different numerical coefficients in eqs 36, 37, and 39. These modifications only change the critical fields E_1, E_2, and E_3 by a numerical factor but do not alter the phase behavior. Indeed, two critical fields between which a regime of mixed state exists have been found experimentally for a BCP is its hexagonal phase by Russell and co-workers.[10] In their experiment, the threshold field (called here E_2) for transition from the mixed to the fully perpendicular state has no noticeable dependence on surface separation L, in accord with our calculations as shown in Figures 8b and 9b.

When the surface separation L is not an integer or half-integer number of the bulk lamellar period d_0, the phase diagrams are given by Figure 9. While in the $E-\delta$ plane the behavior is only slightly changed, in the $E-L$ plane the border of the parallel state has prominent oscillations with period d_0. Finally, we have not considered the copolymer density undulations as was done by Onuki and Fukuda.[20] These might change the boundary lines between the parallel, perpendicular, and mixed phases.

The main prediction of this paper is the dependence of the transition fields on the block copolymer film thickness L and the phase diagrams of Figure 9. It will also be of interest to check experimentally under what conditions the mixed state exists. In addition, the energy penalty γ_T of the defect created in the film as well as the difference in surface energies of the two blocks, $\sigma = \sigma_{AS} - \sigma_{BS}$, can be deduced in experiment from the measured values of E_1, E_2, and E_3 using eqs 42, 44, and 45.

References and Notes

(1) Park, M.; Harrison, C.; Chaikin, P. M.; Register, R. A.; Adamson, D. H. *Science* **1997**, *276*, 1401.
(2) Ibanescu, M.; Fink, Y.; Fan, S.; Thomas, E. L.; Joannopoulos, J. D. *Science* **2000**, *289*, 415.
(3) Fink, Y.; Winn, J. N.; Fan, S.; Chen, C.; Michel, J.; Joannopoulos, J. D.; Thomas, E. L. *Science* **1998**, *282*, 1679. Urbas, A.; Sharp, R.; Fink, Y.; Thomas, E. L.; Xenidou, M.; Fetters, L. J. *Adv. Mater.* **2000**, *12*, 812.
(4) Leibler, L. *Macromolecules* **1980**, *13*, 1602.
(5) Ohta, T.; Kawasaki, K. *Macromolecules* **1986**, *19*, 2621.
(6) Bates, F. S.; Fredrickson, G. H. *Annu. Rev. Phys. Chem.* **1990**, *41*, 525.
(7) Amundson, K.; Helfand, E.; Quan, X.; Hudson, S. D. *Macromolecules* **1993**, *26*, 2698.
(8) Amundson, K.; Helfand, E.; Quan, X. *Macromolecules* **1994**, *27*, 6559.
(9) Morkved, T.; Lu, M.; Urbas, A. M.; Ehrichs, E. E.; Jaeger, H. M.; Mansky, P.; Russell, T. P. *Science* **1996**, *273*, 931.
(10) Thurn-Albrecht, T.; DeRouchey, J.; Russell, T. P. *Macromolecules* **2000**, *33*, 3250.
(11) Tsori, Y.; Andelman, D. *Eur. Phys. J. E* **2001**, *5*, 605.
(12) Turner, M. S. *Phys. Rev. Lett.* **1992**, *69*, 1788.
(13) Walton, D. G.; Kellogg, G. J.; Mayes, A. M.; Lambooy, P.; Russell, T. P. *Macromolecules* **1994**, *27*, 6225.
(14) Fredrickson, G. H.; Helfand, E. *J. Chem. Phys.* **1987**, *87*, 697.
(15) Tsori, Y.; Andelman, D. *Europhys. Lett.* **2001**, *53*, 722.
(16) Tsori, Y.; Andelman, D. *Macromolecules* **2001**, *34*, 2719.
(17) Swift, J.; Hohenberg, P. C. *Phys. Rev. A* **1977**, *15*, 319.
(18) Chen, H.; Chakrabarti, A. *J. Chem. Phys.* **1998**, *108*, 6897.
(19) For a calculation which does not assume $\xi \gtrsim L$ refer to: Kyrylyuk, A. V.; Zvelindovsky, A. V.; Sevink, G. J. A.; Fraaije, J. G. E. M. *Macromolecules* **2002**, *35*, 1473.

(20) Onuki, A.; Fukuda, J. *Macromolecules* **1995**, *28*, 8788.
(21) Pereira, G. G.; Williams, D. R. M. *Macromolecules* **1999**, *32*, 8115.
(22) de Gennes, P. G.; Prost, J. *The Physics of Liquid Crystals*; Oxford University: New York, 1993. Helfrich, W. *Appl. Phys. Lett.* **1970**, *17*, 531. Helfrich, W. *J. Chem. Phys.* **1971**, *55*, 839. Hurault, J. P. *J. Chem. Phys.* **1973**, *59*, 2068.
(23) Ashok, B.; Muthukumar, M.; Russell, T. P. *J. Chem. Phys.* **2001**, *115*, 1559.
(24) Brazovskii, S. A. *Sov. Phys. JETP* **1975**, *41*, 85.
(25) Fabre, P.; Casagrande, C.; Veyssie, M.; Cabuil, V.; Massart, R. *Phys. Rev. Lett.* **1990**, *64*, 539.